ELECTROSTATIC DEFLECTOR OF THE CYCLOTRON DC-280 AXIAL INJECTION CHANNEL

N. Kazarinov†, I. Ivanenko
JINR, Dubna, Moscow region, 141980, Russia
† nyk@lnr.jinr.ru

MOPA14

Abstract

The spherical electrostatic deflector will be used in the axial injection channel of the DC-280 cyclotron for rotation of the ion beam onto vertical axis. The results of the simulation of beam dynamics in the deflector based on 3D electrical field map are discussed in this report. The results of simulation of the ion beam transport in the axial injection beam line of the cyclotron are presented also.

INTRODUCTION

The isochronous heavy-ion cyclotron DC-280 is a basic part of the Super Heavy Element Facility – the new accelerator complex of Joint Institute for Nuclear Research [1,2]. The DC-280 cyclotron will produce high-intensity beam of accelerated ions in the range from helium to uranium. The maximum design value of a current of ion beams will be 10 pmcA and the maximum kinetic energy will be 8 MeV/u. The layout of DC-280 cyclotron is shown in Fig.1.

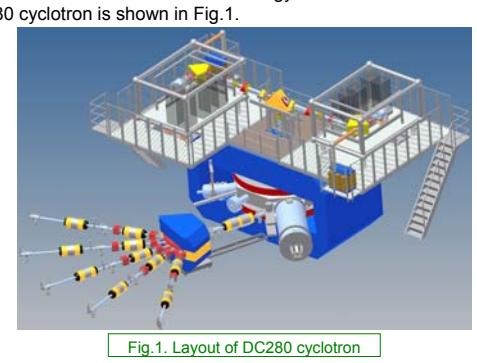

Fig.1. Layout of DC280 cyclotron

In this report the design of the spherical electrostatic deflector of high voltage injection system [2, 3] of DC-280 cyclotron is presented. Using the electrostatic deflector is explained both weight reduction and lower power of the power supply system in comparison with the bending magnet. The design is based on three-dimensional calculation of the magnet field carried out by using OPERA 3D program code [4].

The 3D macro-particle beam dynamic simulation in the deflector was done in the curvilinear coordinates system connected with reference orbit, defined for computational field map. This simulation was carried out by using MCIB04 program code [5].

3D PHYSICAL MODEL OF DEFLECTOR

3D physical model of electrostatic deflector is shown in Fig.2.

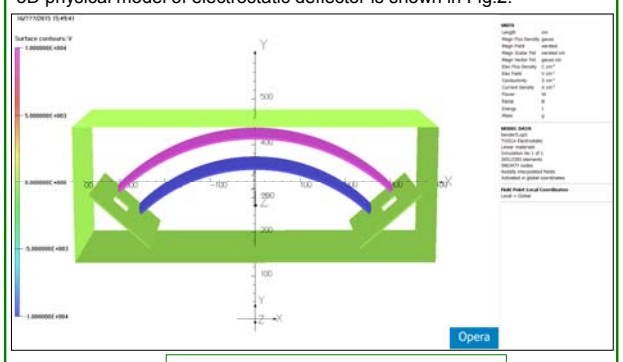

Fig.2. Physical model of spherical deflector.

Deflector consists of two electrodes under the potentials -U1 (blue colour), U2 (red colour) and three ground electrodes (green colour). The design bending radius R=40 cm, the gap between the electrodes d=6 cm, the width of the electrodes h=16 cm. The electric field map consists of two potential distributions $\Phi_{1,2}$ corresponding to the following combinations of voltages at the electrodes (U1=10kV,U2=0) and (U1=0,U2=10kV). The resulting field map of the deflector Φ is a superposition of these distributions:

$$\Phi(\vec{r}) = \left[U_2\Phi_2(\vec{r}) - U_1\Phi_1(\vec{r})\right]\times 10^{-4}$$

The design orbit of the deflector is shown in Fig.3. Voltage U distribution along the design orbit in the case U1,2 =12kV is shown in Fig.4.

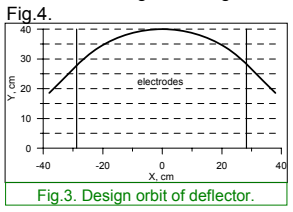

Fig.3. Design orbit of deflector.

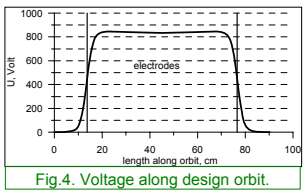

Fig.4. Voltage along design orbit.

The dependences of the components $E_{X,Y}$ of the electric field on distance s along the design orbit of the deflector are shown in Fig.5,6.

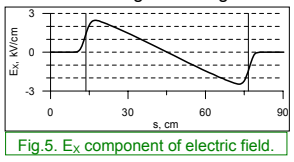

Fig.5. E_X component of electric field.

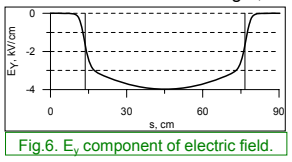

Fig.6. E_y component of electric field.

CALCULATED EQUILIBRIUM ORBIT

The particle motion at the equilibrium orbit of the deflector $[X_0(s_c),Y_0(s_c)]$ is completely determined by two functions– the curvature of the orbit $K_0(s_c)$ and "friction coefficient" $\Lambda_0(s_c)$, depending on length along orbit s_c:

$$K_0(s_c) = -\frac{E_n(s_c)}{(B\rho\beta)_0}$$

$$\Lambda_0(s_c) = \frac{E_t(s_c)}{(B\rho\beta)_0}$$

$$X_0'' = K_0(s_c)Y_0'$$

$$Y_0'' = -K_0(s_c)X_0'$$

$$\frac{(B\rho\beta_0)'}{B\rho\beta_0} = (2-\beta_0^2)\Lambda_0(s_c)$$

Here $E_{n,t}$ – are normal and tangent components of the electric field at the equilibrium orbit; $B\rho_0$ and β_0 – are magnetic rigidity and relativistic velocity of the reference particle, respectively. Prime denotes differentiations with respect to s_c.

Calculated equilibrium orbit is found by varying the voltage U1,2 at electrodes and the radius of the orbit in the middle point. The matching conditions are the coincidence of the coordinates and angles of the calculated and design orbit at the edge of the field map and a minimum of rms deviation between the two orbits. For injection voltage Uinj=80 kV the values of voltages are equal to U1=12.2 kV and U2=11.7 kV. The calculated equilibrium (solid line) and design (dashed line) orbits are shown in Fig.7. Deviation Δ between calculated and designed orbits is shown in Fig.8.

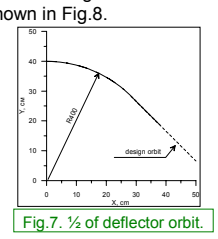

Fig.7. ½ of deflector orbit.

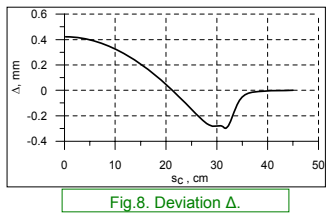

Fig.8. Deviation Δ.

The dependences of the voltage U, normal E_n and tangent E_t components of the electric field on distance s_c along the calculated equilibrium orbit of the deflector are shown in Fig.9-11.

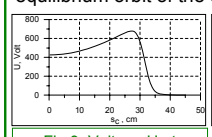

Fig.9. Voltage U at calculated equilibrium orbit

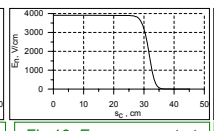

Fig.10. E_n component at calculated equilibrium orbit

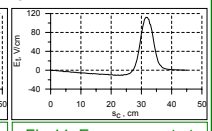

Fig.11. E_t component at calculated equilibrium orbit

BEAM FOCUSING IN THE DEFLECTOR

The simulation of the dynamics of the ions in the deflector is convenient to carry out in the natural system of the coordinate (x,z,s_c) (see Fig.12) associated with calculated equilibrium orbit $[X_0(s_c),Y_0(s_c)]$. The equation for the radius-vector of the particle $\boldsymbol{r}$ in this coordinate system has a form:

$$\boldsymbol{r}'' = \left(\frac{\beta'}{\beta} - \frac{\beta_0'}{\beta_0}\right)\boldsymbol{r}' + \frac{1}{B\rho\beta}\left[\left(\frac{\beta}{\beta_0}\right)^2\vec{E} - (\boldsymbol{r}'\boldsymbol{E})\boldsymbol{r}'\right]$$

$$(B\rho\beta)' = [2-\beta^2](\boldsymbol{r}'\boldsymbol{E})$$

$$\frac{\beta}{\beta_0} = \sqrt{(1+K_0x)^2 + x'^2 + z'^2}$$

$$\boldsymbol{r} = (X_0 - xY_0', Y_0 + xX_0', z);\ \boldsymbol{E} = (E_n, E_s, E_t) =$$

$$= (-E_xY_0' + E_YX_0', E_z, E_xX_0' + E_YY_0')$$

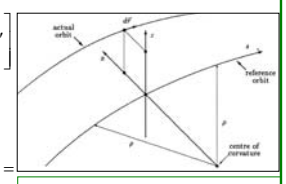

Fig.12. Natural coordinate system

All the components of the electric field vector $\boldsymbol{E}$ should be evaluated by using the electric field map at the location $\boldsymbol{r}$ of the particle.

The linear approximation of the equations of motion defines the focusing properties of the deflector.

$$x'' = -\Lambda_0x' - (3-\beta_0^2)K_0^2x + \frac{1}{(B\rho\beta)_0}\frac{\partial E_n}{\partial x}x + 2\frac{\Delta M}{M_0}K_0$$

$$z'' = -\Lambda_0z' + \frac{1}{(B\rho\beta)_0}\frac{\partial E_z}{\partial z}z$$

$$\Delta M / M_0 = \Delta p / p_0 + K_0x$$

$$(\Delta M / M_0)' = -(2-\beta_0^2)\Lambda_0(\Delta M / M_0)$$

$$(\Delta M / M_0)(B\rho\beta)_0 = const$$

SPHERICAL DEFLECTOR

$$K_0 = \frac{1}{R};\ \Lambda_0 = 0$$

$$\frac{\partial E_n}{\partial x} = -2\frac{E_n}{R};\ \frac{\partial E_z}{\partial z} = \frac{E_n}{R}$$

$$x'' = -\frac{1-\beta_0^2}{R^2}x + \frac{2}{R}\frac{\Delta M}{M_0}$$

$$z'' = -\frac{1}{R^2}z$$

$$\frac{\Delta M}{M_0} = \left(\frac{\Delta p}{p_0}\right)_{in} = const$$

CYLINDRICAL DEFLECTOR

$$K_0 = \frac{1}{R};\ \Lambda_0 = 0$$

$$\frac{\partial E_n}{\partial x} = -\frac{E_n}{R};\ \frac{\partial E_z}{\partial z} = 0$$

$$x'' = -\frac{2-\beta_0^2}{R^2}x + \frac{2}{R}\frac{\Delta M}{M_0}$$

$$z'' = 0$$

$$\frac{\Delta M}{M_0} = \left(\frac{\Delta p}{p_0}\right)_{in} = const$$

Here $(\Delta p/p)_{in}$ – is the momentum spread at the entrance of the deflector.

In the spherical electrostatic deflector the focusing terms are approximately the same both for x- and z- motions. In the cylindrical electrostatic deflector the focusing term is absent for z- motion.

EDGE FIELD. SHIFTED ORBIT REGIME

The simulation of the beam focusing in the field map of the spherical deflector by using the linear equations of motion shows the significant asymmetry of the beam envelopes at the exit of the deflector (see Fig.13). This asymmetry is caused by edge field and may be minimized by shifting the equilibrium orbit towards the inner electrode of the deflector (see Fig.14). The entrance and the exit points of the orbit do not changed during this shifting (see Fig.15).

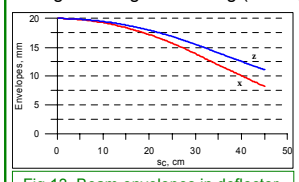

Fig.13. Beam envelopes in deflector.

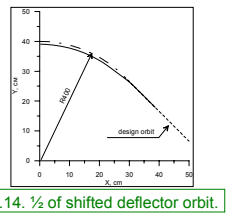

Fig.14. ½ of shifted deflector orbit.

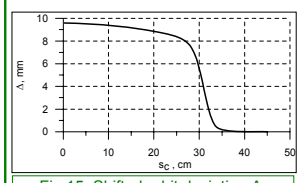

Fig.15. Shifted orbit deviation Δ.

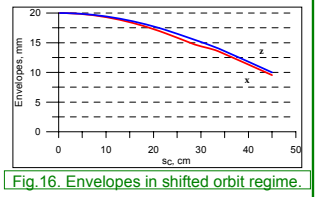

Fig.16. Envelopes in shifted orbit regime.

In this regime the value of the voltage at the electrodes U1 =16.6 kV strongly differs from U2 =8.9 kV (in the case of maximum injection voltage U_{inj} = 80 kV). The maximum deviation of the shifted equilibrium orbits from the design one is about 10 mm. The difference between x- and z-envelopes at the exit of deflector is less than 1mm (see Fig.16).

The dependences of the voltage U, normal E_n and tangent E_t components of the electric field on distance s_c along the shifted orbit of the deflector are shown in Fig.17-19.

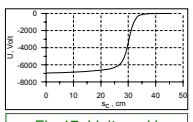

Fig.17. Voltage U at shifted orbit

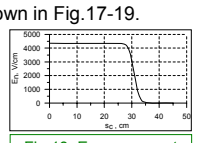

Fig.18. E_n component at shifted orbit

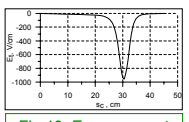

Fig.19. E_t component at shifted orbit

BEAM TRANSPORT THROUGH DEFLECTOR

The macro particle simulation of the ion beam transport through the deflector by using the nonlinear equation of motion verified the possibility of the correction of the beam focusing asymmetry. The beam envelopes and the beam emittance during transportation are shown in Fig.20,21. The ion distributions at various phase planes in the final point of transportation are shown in Fig.22-24. Dew to axial symmetry of the beam the nonlinear distortions of the emittance are negligibly small.

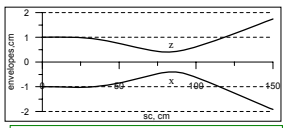

Fig.20. Beam envelopes.

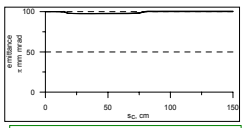

Fig.21. Beam emittance.

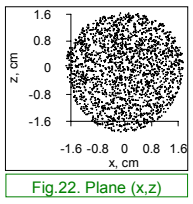

Fig.22. Plane (x,z)

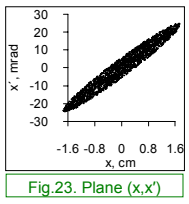

Fig.23. Plane (x,x')

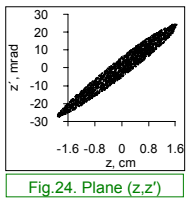

Fig.24. Plane (z,z')

DC-280 AXIAL INJECTION CHANNEL

The scheme of the high voltage axial injection beam line of DC-280 cyclotron is shown in Fig.25.

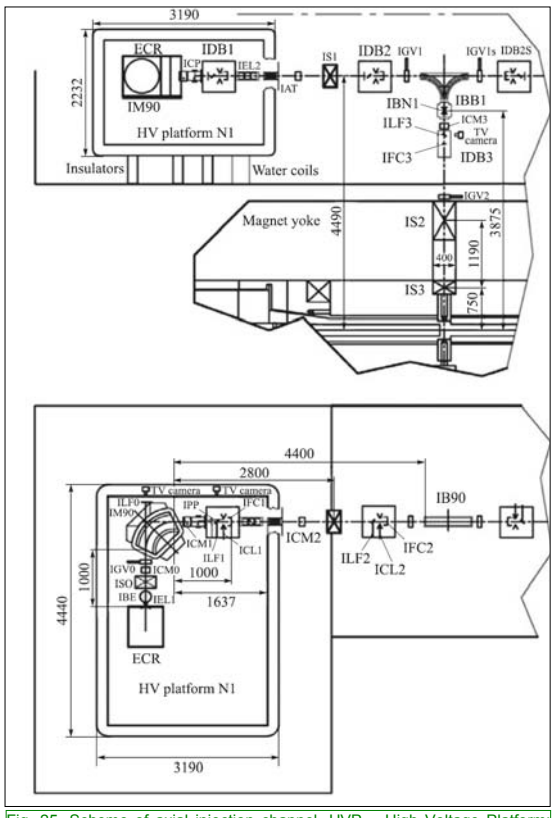

Fig. 25. Scheme of axial injection channel. HVP – High Voltage Platform; ECR – ECR ion source; IS0-3 – focusing solenoids; IM90 – analyzing magnet; IEL1,2 electrostatic lenses; IAT – acceleration tube; IBD90 – spherical electrostatic deflector.

The ion beam is extracted from ECR ion source with energy 25 keV/Z. After analyzing and separation in the IM90 magnet the beam is accelerated in IAT tube. The kinetic beam energy may be increased by acceleration up to 80 keV/Z. All these equipment is placed at High Voltage Platform HVP. The electrostatic deflector IB90 rotates the beam onto vertical axis and two solenoids IS2,3 match the beam emittance with acceptance of the cyclotron inflector.

In the numerical simulation of the ion beam dynamics in the axial injection beam line 3D field maps of analyzing magnet IM90 [6], solenoids IS0-3, acceleration tube IAT and spherical electrostatic deflector IB90 are used.

The transport of 48Ca8+ ion beam with kinetic energy of 75 keV/Z is considered. The efficiency of the beam transport is equal to 100%.

The dependence of the beam envelopes on length along the channel are shown in Fig.26. The beam envelopes in the magnetic plug and inflector of the cyclotron are shown in Fig.27.

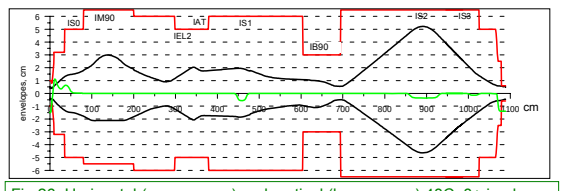

Fig.26. Horizontal (upper curve) and vertical (lower curve) 48Ca8+ ion beam envelopes, aperture (red lines), longitudinal magnetic field (green line).

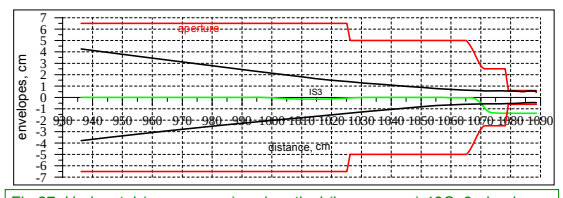

Fig.27. Horizontal (upper curve) and vertical (lower curve) 48Ca8+ ion beam envelopes in magnetic plug and inflector of the cyclotron.

The dependence of the kinetic energy of the beam W on the length along the beam line is represented in Fig.28. The horizontal (red curve) and vertical (blue curve) beam emittances are shown in Fig.29. The decreasing of the beam emittance is explained by increasing of kinetic energy in the acceleration tube IAT.

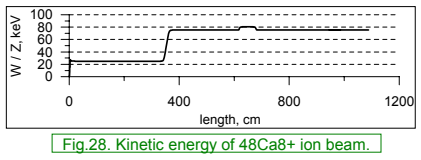

Fig.28. Kinetic energy of 48Ca8+ ion beam.

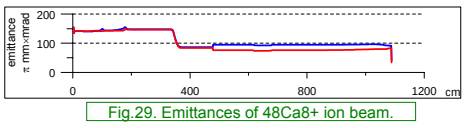

Fig.29. Emittances of 48Ca8+ ion beam.

REFERENCES

[1] G.Gulbekyan, B.Gikal, I.Kalagin, N.Kazarinov. "Status Report and Future Development FLNR JINR Heavy Ions Accelerators Complex", Proceedings of 11-th International Conference on Heavy Ion Accelerators Technology, HIAT09, 8-12 June 2009, Venezia, Italy, p.p. 59-63.

[2] I.Ivanenko, G.Gulbekyan, N.Kazarinov, E.Samsonov, "Injection and Acceleration of Intense Heavy Ion Beams in JINR New Cyclotron DC280", MOA1C02, these proceedings, HIAT 2015, Yokohama, Japan (2015).

[3] G.G. Gulbekyan, V. Bekhterev, S.L. Bogomolov, A.A. Efremov, B. Gikal, I.A. Ivanenko, I.V. Kalagin, N.Yu. Kazarinov, M.V. Khabarov, V.N. Melnikov, N.F. Osipov, S.V. Prokhorov, A. Tikhomirov, "The Project of the HV Axial Injection for the DC-280 Cyclotron at the FLNR JINR", Proceedings of XXIV Russian Accelerator Conference, RuPAC'2014, Obninsk, Russia (2014), p.p. 333-335.

[4] OPERA-3D Reference Manual, Oxford OX5 1JE, England, October 2012

[5] V.Alexandrov, N.Kazarinov, V.Shevtsov, "Multi-Component Ion Beam code – MCIB04". Proceeding of XIX-th Russian Particle Accelerator Conference, RUPAC2004, 4-9 October, Dubna, Russia, p.p.201-203.

[6] N.Yu.Kazarinov, I.A.Ivanenko, "Magnets of Injection and Extraction Systems of Cyclotron DC280". Proceedings of XXIV Russian Accelerator Conference, RuPAC'2014, Obninsk, Russia (2014), p.p. 339-341.